Published in final edited form as:
J Nucl Med. 2007 October ; 48(10): 1724–1732. doi:10.2967/jnumed.107.040279.

PET Studies of *d*-Methamphetamine Pharmacokinetics in Primates: Comparison with *l*-Methamphetamine and (—)-Cocaine

Joanna S. Fowler[1,3], **Carsten Kroll**[4], **Richard Ferrieri**[1], **David Alexoff**[1], **Jean Logan**[1], **Stephen L. Dewey**[1], **Wynne Schiffer**[1], **David Schlyer**[1], **Pauline Carter**[1], **Payton King**[1], **Colleen Shea**[1], **Youwen Xu**[1], **Lisa Muench**[5], **Helene Benveniste**[1,6], **Paul Vaska**[1], and **Nora D. Volkow**[5,7]

[1]Brookhaven National Laboratory, Upton, New York [2]Mount Sinai School of Medicine, New York, New York [3]Department of Chemistry, State University of New York at Stony Brook, Stony Brook, New York [4]University of Mainz, Mainz, Germany [5]National Institute on Alcoholism and Alcohol Abuse, Rockville, Maryland [6]Department of Anesthesiology, Health Sciences Center, State University of New York at Stony Brook, Stony Brook, New York [7]National Institute on Drug Abuse, Rockville, Maryland

Abstract

The methamphetamine molecule has a chiral center and exists as 2 enantiomers, *d*-methamphetamine (the more active enantiomer) and *l*-methamphetamine (the less active enantiomer). *d*-Methamphetamine is associated with more intense stimulant effects and higher abuse liability. The objective of this study was to measure the pharmacokinetics of *d*-methamphetamine for comparison with both *l*-methamphetamine and (—)-cocaine in the baboon brain and peripheral organs and to assess the saturability and pharmacologic specificity of binding.

Methods—*d*- and *l*-methamphetamine and (—)-cocaine were labeled with ^{11}C via alkylation of the norprecursors with ^{11}C-methyl iodide using literature methods. Six different baboons were studied in 11 PET sessions at which 2 radiotracer injections were administered 2–3 h apart to determine the distribution and kinetics of ^{11}C-*d*-methamphetamine in brain and peripheral organs. Saturability and pharmacologic specificity were assessed using pretreatment with *d*-methamphetamine, methylphenidate, and tetrabenazine. ^{11}C-*d*-Methamphetamine pharmacokinetics were compared with ^{11}C-*l*-methamphetamine and ^{11}C-(—)-cocaine in both brain and peripheral organs in the same animal.

Results—^{11}C-*d*- and *l*-methamphetamine both showed high uptake and widespread distribution in the brain. Pharmacokinetics did not differ between enantiomers, and the cerebellum peaked earlier and cleared more quickly than the striatum for both. ^{11}C-*d*-Methamphetamine distribution volume ratio was not substantially affected by pretreatment with methamphetamine, methylphenidate, or tetrabenazine. Both enantiomers showed rapid, high uptake and clearance in the heart and lungs and slower uptake and clearance in the liver and kidneys. A comparison of ^{11}C-*d*-methamphetamine and ^{11}C-(—)-cocaine showed that ^{11}C-*d*-methamphetamine peaked later in the brain than did ^{11}C-(—)-cocaine and cleared more slowly. The 2 drugs showed similar behavior in all peripheral organs examined except the kidneys and pancreas, which showed higher uptake for ^{11}C-*d*-methamphetamine.

For correspondence or reprints contact: Joanna S. Fowler, PhD, Medical Department, Bldg. 555, Brookhaven National Laboratory, P.O. Box 5000, Upton, NY 11973. E-mail: fowler@bnl.gov.

Conclusion—Brain pharmacokinetics did not differ between *d*-and *l*-methamphetamine and thus cannot account for the more intense stimulant effects of *d*-methamphetamine. Lack of pharmacologic blockade by methamphetamine indicates that the PET image represents nonspecific binding, though the fact that methamphetamine is both a transporter *substrate* and an *inhibitor* may also play a role. A comparison of ^{11}C-*d*-methamphetamine and ^{11}C-(—)-cocaine in the same animal showed that the slower clearance of methamphetamine is likely to contribute to its previously reported longer-lasting stimulant effects relative to those of (—)-cocaine. High kidney uptake of *d*-methamphetamine or its labeled metabolites may account for the reported renal toxicity of *d*-methamphetamine in humans.

Keywords

PET; methamphetamine; ^{11}C; brain; peripheral organs

Methamphetamine is a highly addictive stimulant drug that is toxic to brain and peripheral organs (1). It is both a substrate and an inhibitor of monoamine transporters releasing dopamine and other neurotransmitters through the individual neurotransmitter transporters on the presynaptic neurons and on intracellular vesicles (1). It has been shown to be neurotoxic to laboratory animals at doses that are self-administered in human abusers (2). Its chronic use also leads to structural abnormalities (3) and evidence of dopamine terminal damage in the brains of living human methamphetamine abusers (4,5). In addition to its addictive and toxic properties, methamphetamine abuse is also associated with risky sexual behavior that facilitates HIV infection (6).

The methamphetamine molecule has a chiral center and exists as 2 enantiomers, *d*-methamphetamine (*S*-(+)-*N*-*α*-dimethylphenethylamine) and *l*-methamphetamine (*R*-(—)-*N*-*α*-dimethylphenethylamine). The 2 enantiomers differ in their physiologic and pharmacologic potency, with the *d*-enantiomer generally being associated with more potent physiologic and behavioral effects and higher abuse liability (7). The *d*-enantiomer is also a more potent dopamine releaser. A microdialysis study in rats, comparing dopamine elevation by *d*- and *l*-methamphetamine, found that *d*-methamphetamine elevated dopamine by 650% at a dose of 2 mg/kg whereas *l*-methamphetamine elevated dopamine by only 250% at a much larger dose of 12 mg/kg (8).

d-Mehamphetamine is readily synthesized by reduction of pseudoephedrine. It is the form that is the most commonly produced in clandestine laboratories and thus is the form that is the most commonly abused. In the past, methamphetamine was commonly synthesized as the racemic mixture from phenylacetone as one of the main chemical precursors, and thus, human exposure to the *l*-enantiomer was of pharmacologic and toxicologic relevance (9). It is noteworthy that *d*-methamphetamine is currently marketed as Desoxyn (Abbott Laboratories) for the treatment of attention deficit disorder and exogenous obesity and that *l*-methamphetamine is a component of the over-the-counter Vicks Vapor Inhaler (Procter & Gamble).

^{11}C-*d*,*l*-Methamphetamine and its individual labeled enantiomers have been synthesized by ^{11}C-methylation of *d*,*l*-amphetamine and its individual enantiomers with ^{11}C-methyl iodide (10). Biodistribution studies on mice showed that both enantiomers entered the mouse brain and heart and cleared according to a single exponential curve. Brain uptake was decreased by treatment with reserpine, which blocks the vesicular monoamine transporter (VMAT). Several PET studies on monkeys and dogs have measured the pharmacokinetics of ^{11}C-labeled racemic methamphetamine and either *d*- or *l*-methamphetamine. For example, PET studies with ^{11}C-*l*-methamphetamine on rhesus monkeys showed no difference in uptake between different brain regions, indicating that the binding is nonspecific (11). Mizugaki et al. reported differences in ^{11}C-methamphetamine uptake with different anesthetics (12), and though the authors did

not specify the enantiomeric form, earlier studies in this same group studied methamphetamine sensitization using the active enantiomer, ^{11}C-*d*-methamphetamine (13).

To our knowledge, direct comparison of the pharmacokinetics of *d*- and *l*-methamphetamine in different regions of the brain and in the peripheral organs of baboons has not been reported, nor has the saturability and pharmacologic specificity of the *d*-enantiomer been assessed. Because high uptake and rapid brain entry of drug is crucial in stimulant reinforcement, and because peripheral organ toxicity is also a concern, we set out, first, to determine whether brain uptake and kinetics are consistent with the more intense stimulant effects of *d*-methamphetamine relative to *l*-methamphetamine; second, to identify target organs for methamphetamine and its labeled metabolites; third, to assess the brain saturability and pharmacologic specificity of *d*-methamphetamine; and fourth, to directly compare the pharmacokinetics of ^{11}C-*d*-methamphetamine and ^{11}C-(—)-cocaine in the brain and peripheral organs of the same animal.

MATERIALS AND METHODS

Baboon Preparation

All animal studies were reviewed and approved by the Brookhaven Institutional Animal Use and Care Committee. Six different baboons were studied in 11 PET sessions in which 2 radiotracers were administered 2 h apart. The baboons were anesthetized with a dose of ketamine (10 mg/kg); intubated and ventilated with a mixture of isoflurane (1%–4%, Forane; Baxter Healthcare Corp.), nitrous oxide (1,500 mL/min), and oxygen (800 mL/min); and then catheterized for radiotracer injection and arterial sampling as described previously (14). The baboon studies and details on drug administration are summarized in Table 1.

PET Studies

^{11}C-*d*- and *l*-methamphetamine were prepared from *d*- and *l*-amphetamine and ^{11}C-methyl iodide according to the method of Inoue et al. (10). *d*-Amphetamine was obtained from K & K Laboratories, and *l*-amphetamine was obtained from Sigma-Aldrich. Dynamic PET was performed on a Siemens HR+ high-resolution, whole-body PET scanner (4.5 × 4.5 × 4.8 mm at the center of the field of view) in 3-dimensional acquisition mode, using 63 planes. For all scans (brain and body), a transmission scan was obtained with a ^{68}Ge rotating rod source before radiotracer injection for each emission scan to correct for attenuation. The specific activity of ^{11}C-*d*- or *l*-methamphetamine ranged from 18 to 37 GBq/μmol (0.5–1.0 Ci/μmol at the end of synthesis), and the dose injected ranged from 74 to 148 MBq (2–4 mCi). The radiochemical purity was greater than 98%. Scanning was performed for 90 min with the following time frames (1 × 10 s, 12 × 5 s, 1 × 20 s, 1 × 30 s, 8 × 60 s, 4 × 300 s, and 8 × 450 s). Typically, 2 studies were performed 2 h apart on each scanning day to compare enantiomers, to assess the effect of pharmacologic intervention, or to compare ^{11}C-*d*-methamphetamine with ^{11}C-(—)-cocaine. In the case of tetrabenazine pretreatment studies, there was a 3-h interval between injections.

^{11}C-(—)-Cocaine was synthesized from norcocaine (NIDA Research Technology Branch) according to the literature method (15). Radiochemical purity was greater than 98%, and specific activity was 18–92 GBq/μmol (0.2–2.5 Ci/μmol at the end of synthesis). Scanning was performed for 54 min with the following time frames (1 × 10 s, 12 × 5 s, 1 × 20 s, 1 × 30 s, 4 × 60 s, 4 × 120 s, and 8 × 300 s).

Image Analysis

Time frames were summed over the experimental period (90 min for ^{11}C-*d*- and *l*-methamphetamine and 54 min for ^{11}C-(—)-cocaine), and planes were summed in groups of 2

for the purpose of region-of-interest (ROI) placement. ROIs were placed over the striatum and the cerebellum and then projected onto the dynamic images to obtain time—activity curves. For ^{11}C-*d*- and *l*-methamphetamine, ROIs were also placed on the thalamus, frontal cortex, and temporal cortex. For both labeled compounds, a global ROI was placed over 3 central planes. Regions occurring bilaterally were averaged. The ^{11}C concentration in each ROI was divided by the injected dose to obtain the percentage injected dose (%ID)/cm^3. A similar strategy was used for ROI placement for peripheral organs, in which we chose regions on the heart, lungs, liver, kidneys, pancreas, and spleen. For 3 baboon studies in which ^{11}C-*d*-and *l*-methamphetamine were compared in the same animal, we compared the peak uptake (%ID)/cm^3, time to reach peak uptake, clearance half-time from peak for the striatum and the cerebellum, distribution volume ratio (DVR; striatum to cerebellum), and plasma integral (uncorrected and corrected for the presence of labeled metabolites) using the paired *t* test, 2-tailed. Clearance half-time from peak was determined by inspecting each time—activity curve and determining the difference in time between the time at peak and the time at which the radioactivity concentration decreased by 50%. For the studies comparing baseline and drug administration (Table 1) in the same animal, we compared time—activity curves and the striatum-to-cerebellum DVR using graphical analysis (Logan plot) (16). For studies comparing ^{11}C-*d*-methamphetamine and ^{11}C-(—)-cocaine, we compared time—activity data for the brain and peripheral organs and DVRs for the brain.

Plasma Analysis for Fraction of ^{11}C-Methamphetamine

Radioactivity in plasma samples from the baboons was measured in a calibrated well counter. Plasma, sampled at 7 different time points, was analyzed manually by high-performance liquid chromatography and automatically by solid-phase extraction using a laboratory robot (Zymark/Caliper Life Sciences) as previously described (17). High-performance liquid chromatography conditions were modified from the literature procedure to optimize the separation of 4-hydroxymethamphetamine from methamphetamine and its other potentially labeled metabolites and to verify that the solid-phase method separated the 4-hydroxy metabolite from methamphetamine. Plasma samples were analyzed using a Spherisorb ODS1 5-μm column (Waters) (80:20 MeOH:0.1 M ammonium formate with 1 mL of triethylamine solvent; 1.2 mL/min). Retention times were 4.5 and 7 min for 4-hydroxymethamphetamine and methamphetamine, respectively. High-performance liquid chromatography analysis was used only to validate the robot solid-phase extraction methodology. The total radioactivity concentration in plasma for each subject for each scan was corrected for the presence of labeled metabolites determined by solid-phase extraction to obtain the input function that was used in distribution volume estimation.

Log D Determination

A modification of a literature procedure was used (18). Briefly, an aliquot (50 μL) of ^{11}C-methamphetamine or ^{11}C-(—)-cocaine solution was added to a mixture of 1-octanol (2.5 mL) and phosphate-buffered saline (pH 7.4; 2.5 mL). The mixture was stirred in a vortex mixer at room temperature for 2 min and then centrifuged at 7,000 rpm for 2 min. An aliquot (0.1 mL) of the octanol layer and 1.0 mL of the buffer layer were sampled separately into 2 empty vials and counted. Two milliliters of the octanol layer were transferred into a test tube containing 0.5 mL of fresh octanol and 2.5 mL of buffer, the process of stirring and centrifuging was repeated, and the aliquots from each layer were extracted and counted until 6 measures of the ratio of counts in the octanol to counts in the buffer were obtained. Log D is the log (base 10) of the average of the ratios of the decay-corrected counts in the octanol—buffer mixture.

Measurement of Free Fraction of ^{11}C-*d*-Methamphetamine in Plasma

The radioactivity in an aliquot of ^{11}C-*d*- and *l*-methamphetamine solution was measured in a well counter and added to 500 μL of baboon plasma, and this was incubated for 10 min at room temperature. Aliquots (20–40 μL) of the incubated spike plasma were counted (unspun aliquot). Two hundred to 400 μL of the incubation mixture were placed in the upper level of a Centrifree tube (Amicon Inc.), and this was centrifuged at 2,000*g* for 10 min, during which time the temperature of the sample did not change. After centrifuging, the top portion of the Centrifree tube, containing the bound portion, was removed and discarded, and precisely measured aliquots (20–40 μL) of the liquid in the cup (unbound aliquot) were counted. The free fraction is the ratio of the decay-corrected counts of the unbound aliquots to the decay-corrected counts of the unspun aliquots.

RESULTS

d- and *l*-Methamphetamine Rapidly Distributes to Subcortical and Cortical Brain Regions

Both ^{11}C-*d*- and *l*-methamphetamines had high, rapid, and widespread uptake in both subcortical and cortical brain regions, consistent with its measured log D (-0.38 ± 0.01; range, -0.35 to -0.40) (19) and a large (80%) free fraction in plasma for both enantiomers. A coregistered brain image of ^{11}C-*d*-methamphetamine (summed frames over 90 min) is shown in Figure 1. Time—activity curves are shown in Figure 2 for one of the baboons to whom both enantiomers were administered in the same scanning session. Figure 1 shows that ^{11}C was present throughout the brain, and Figure 2 shows that the peak times and clearance rates for most brain regions were similar except for the cerebellum, which peaked earlier and cleared more rapidly for both enantiomers (Fig. 2; Table 2). There was essentially no difference in the PET measurements between the *d*- and *l*-enantiomers in peak uptake, time to peak, or DVR (Table 2). The plasma clearance of ^{11}C showed a trend toward being slower (trend $P < 0.08$) for the *d*- than the *l*-enantiomer (as reflected by the integral at 60 min, Table 2). However, when corrected for the fraction of total radioactivity as ^{11}C-methamphetamine (which was significantly lower for ^{11}C-*d*-methamphetamine than for ^{11}C-*l*-methamphetamine [Table 3]), there was no significant difference between the plasma input for the *d*- and *l*-enantiomers (49,876 ± 1,221 vs. 50,208 ± 1,887 Bq/mL × min, respectively).

d- and *l*-Methamphetamine Show Similar Distribution and Kinetics in Peripheral Organs, with Highest Accumulation in Kidneys and Liver

Both ^{11}C-*d*-and *l*-methamphetamines showed rapid uptake and clearance from the heart, lungs, and spleen, with ^{11}C being retained slightly longer in the spleen than in the heart and lungs (Fig. 3). In contrast, both enantiomers showed high uptake and relatively slow clearance of ^{11}C from the kidneys and the liver. The rank-order half-time for clearance from peak uptake for both enantiomers was lung > > heart > spleen >> kidneys >> liver.

d-Methamphetamine Accumulation and Clearance Are Not Affected by Methamphetamine, Methylphenidate, or Tetrabenazine Pretreatment

To assess whether *d*-methamphetamine binding in vivo in baboon brain is saturable and specific for the dopamine and norepinephrine transporters or VMAT, we performed serial studies on the same baboon at baseline and after pretreatment with *d*-methamphetamine (0.2 mg/kg, 5 min prior), with methylphenidate (which binds to the dopamine and norepinephrine transporters, 0.5 mg/kg, 10 min prior (21)), and with tetrabenazine (which binds to the VMAT, 4 mg/kg, 60 min prior). We also assessed binding reproducibility in 1 animal with no drug treatment. There was no change in either the time—activity curves (data not shown) or the DVR (Table 4) for the striatum and cerebellum with either *d*-methamphetamine or methylphenidate pretreatment. Though tetrabenazine pretreatment reduced ^{11}C uptake in both

the striatum and the cerebellum (data not shown), the plasma input of radiotracer was also lower and the striatum-to-cerebellum DVR was not substantially changed (Table 4). We noted that the administered dose of tetrabenazine was previously found to elevate synaptic dopamine in the baboon as shown by a change in ^{11}C-raclopride binding (22).

d-Methamphetamine and (—)-Cocaine Differ in Brain Distribution and Kinetics in Brain and in Peripheral Organs

The brain distribution, kinetics, and clearance rates were very different between ^{11}C-*d*-methamphetamine and ^{11}C-(—)-cocaine when compared in the same animal. In contrast to *d*-methamphetamine, (—)-cocaine was localized almost exclusively in the striatum, as shown in Figures 1 (coregistered images for ^{11}C-*d*-methamphetamine and ^{11}C-(—)-cocaine) and 4 (time—activity curves in the striatum and cerebellum). The striatum-to-cerebellum DVR was 1.7 for ^{11}C-(—)-cocaine and 1.22 for ^{11}C-*d*-methamphetamine for the baboon in whom both tracers were injected. (—)-Cocaine peaked earlier than *d*-methamphetamine in the striatum (3.5 vs. 8.0 min) and in the cerebellum (1.75 vs. 5.5 min) and also cleared more rapidly from the striatum (18- vs. 56-min half-time from peak) and the cerebellum (9- vs. 51-min half-time from peak). The total brain uptake at the time of peak uptake was 4.3% and 5.0% for *d*-methamphetamine and (—)-cocaine, respectively.

In peripheral organs, the major difference between the 2 stimulant drugs was the high accumulation and slow clearance from the kidneys seen after injection of ^{11}C-*d*-methamphetamine but not after ^{11}C-(—)-cocaine (Fig. 5). Also, ^{11}C-*d*-methamphetamine had higher uptake in the pancreas than did ^{11}C-(—)-cocaine. On the other hand, the heart and lungs showed similarly rapid clearance—and the liver, slow accumulation and clearance—of ^{11}C for both ^{11}C-*d*-methamphetamine and ^{11}C-(—)-cocaine.

DISCUSSION

Striatal uptake of methamphetamine, its interactions with the plasma dopamine transporter and VMAT, and the consequent large vesicular release of dopamine are believed to be responsible for the intense reinforcing effects of the drug. Here, we have shown that *d*-methamphetamine uptake into the baboon brain is relatively rapid, with peak uptake in the striatum occurring approximately 7 min after injection. For drugs of abuse, rapid brain uptake is associated with reinforcement because the rate at which drugs of abuse increase dopamine modulates their reinforcing effects. The increases in dopamine must occur quickly to be perceived as reinforcing (23).

d-Methamphetamine is also widely distributed in both subcortical and cortical brain regions as can be seen in the time—activity curves in Figure 2 and in the image in Figure 1. Widespread distribution to different brain regions and slow clearance may play a role in the neurotoxicity of methamphetamine because of its access to different populations of neurons, where it has the potential to release transmitters from vesicular stores.

Despite the fact that *d*-methamphetamine induces a significantly higher release of striatal dopamine in rats (8) and is a more powerful stimulant in humans (7), we did not see any difference in pharmacokinetics between ^{11}C-*d*- and *l*-methamphetamine. Thus, factors other than a difference in brain pharmacokinetics must account for the more intense stimulant effects of *d*-methamphetamine.

Though methamphetamine is known to interact with the dopamine transporter and VMAT, releasing large amounts of dopamine (8,24), ^{11}C-methamphetamine uptake was not blocked by either methamphetamine itself or methylphenidate (a stimulant drug that binds to the dopamine and norepinephrine transporters (25)) or by tetrabenazine (a drug that blocks

VMAT). This finding indicates that the PET image is dominated by nonspecific binding. We note that many labeled drugs and other labeled compounds that have pharmacologic specificity for a molecular target do not show specific binding to that target when they are imaged because they also bind to other sites (nonspecific and nontarget) and this other binding overwhelms the specific signal. ^{11}C-Nicotine is another example. There is no doubt that nicotine binds to nicotine receptors in the brain, as can be demonstrated by its pharmacologic activity and by observing the ability of unlabeled nicotine to displace a radiotracer with specificity for the nicotinic acetylcholine receptor (26). However, ^{11}C-nicotine cannot be blocked by unlabeled nicotine because it binds to many other nonspecific sites and the signal is lost in the noise. Similarly, ^{11}C-methamphetamine binding cannot be blocked by unlabeled methamphetamine because it also binds to nonspecific sites that dominate the image.

We compared *d*-methamphetamine and (—)-cocaine in the same animal in both the brain and the peripheral organs to see if differences in their pharmacokinetics could account for differences in their behavioral and toxic effects. The peak striatal uptake was faster for (—)-cocaine than for methamphetamine (3.5 vs. 7 min, respectively), and the clearance rates were also much faster for (—)-cocaine than for *d*-methamphetamine (Fig. 4) (15). This result is consistent with differences in the self-reported temporal course of a “high” between these 2 drugs. Whereas for methamphetamine the peak behavioral effects occur at about 15 min, with a half-time of about 45 min (27), for (—)-cocaine peak effects occur at about 4 min, with a half-time of about 20 min (23). The peak striatal uptake for (—)-cocaine was also higher than the striatal uptake for *d*-methamphetamine, as may be accounted for by the higher log D for cocaine relative to that of *d*-methamphetamine (1.31 ± 0.03 vs. -0.38 ± 0.01) (Fig. 4). Prior studies have shown that ^{11}C-(—)cocaine binds to the dopamine transporter (28), as demonstrated by blockade of striatal uptake by drugs that block the dopamine transporter, contrasting with uptake of methamphetamine, which cannot be blocked and thus represents nonspecific binding.

Because the PET image provides no direct information on the chemical form of the ^{11}C in the brain, there is a question of whether we are observing in the brain the kinetics of the drug itself or of a combination of the labeled drug and its labeled metabolites. ^{11}C-*d*- and *l*-methamphetamine are labeled on the *N*-methyl group. Major metabolic pathways for methamphetamine are *N*-demethylation to produce amphetamine, which would not be labeled, and 4-hydroxylation to produce 4-hydroxymethamphetamine (29), which would retain the label. Labeled methanol and carbon dioxide would be produced from *N*-dealkylation and are expected to contribute little to the brain ^{11}C. An examination of the fraction of ^{11}C that is present in the form of parent radiotracer in the brain is not possible in these baboon studies; however, from an analysis of labeled methamphetamine in baboon plasma during the PET study, more than 50% of the parent compound remains for the *d*-enantiomer and more than 70% remains for the *l*-enantiomer at 20 min after intravenous injection (Table 3). Therefore, the major fraction of ^{11}C that is delivered to the brain soon after injection is in the form of the parent compound. Thus, it is highly likely that it is mostly the parent compound that enters the brain soon after injection, when the powerful reinforcing effects of the drug are crucial. This likelihood is supported by the identification of ^{11}C-methamphetamine in mouse brain after the injection of ^{11}C-methamphetamine (10). For (—)-cocaine, all the ^{11}C that is in the brain is in the form of (—)-cocaine because norcocaine, the only (—)-cocaine metabolite that can cross the blood—brain barrier, would not be labeled (30).

In addition to its effects on the brain, methamphetamine toxicity to other organs has been documented. Toxicity is generally associated with oxidative damage, which is associated with high levels of catecholamines induced by the interaction of methamphetamine with neurotransmitter transporters, as well as with other factors such as inflammation (31). In the heart, acute methamphetamine use produces cardiac lesions whereas chronic use is associated

with cardiomyopathy (32,33). We have found that although ^{11}C-*d*-methamphetamine has a high initial distribution to the heart (0.059%/cm^3 at 0.21 min after injection), its residence time in the heart is short: a half-time of approximately 0.5 min from peak. This pattern was similar to that of ^{11}C-(—)-cocaine in the same animal (Fig. 5). ^{11}C-(—)-Cocaine also had a rapid, high uptake and rapid clearance from the heart. This same pattern has been reported in the human heart (34). Though the residence time of (—)-cocaine in the heart is short, prolonged inhibition of the norepinephrine transporter is shown (as assessed by 6-^{18}F-fluoronorepinephrine), demonstrating that the effects of (—)-cocaine on cardiac neurotransmitter activity can persist long after the drug has cleared (35). Further studies are required to determine whether *d*-methamphetamine has a long-lasting pharmacodynamic effect on norepinephrine transporter in the heart. We note that methamphetamine could also affect the heart through central mechanisms.

Methamphetamine has also been reported to produce kidney damage and peroxidative injury in laboratory rats. In both an acute and a chronic model of methamphetamine administration, immunohistochemical markers, renal function markers, and blood ion concentrations indicated cellular damage consistent with pathologic changes seen in autopsy samples from methamphetamine abusers (36,37). As can be seen in Figure 3, the kidney would have the highest exposure of all the organs to methamphetamine and its labeled metabolites, possibly accounting for the previously reported pathologic changes noted in autopsy samples from methamphetamine abusers.

In this study, we also showed a higher accumulation of ^{11}C-methamphetamine in the pancreas, compared with that of ^{11}C-(—)-cocaine (0.036%/cm^3 at peak vs. 0.025%/cm^3 at peak, Fig. 5). This accumulation could reflect nonspecific binding or binding to VMAT2 in the pancreas. The accumulation is relevant because toxicity to the pancreas has been documented both in preclinical studies and in autopsy cases of individuals dying from a methamphetamine overdose (38). Because VMAT2 in the pancreas is located in β-cells of the islets of Langerhans, which are responsible for the synthesis of insulin (39), this may be the mechanism underlying methamphetamine-induced insulin release (40).

An objective of this study was to ask whether the pharmacokinetics of ^{11}C-methamphetamine at a tracer dose would be similar to the pharmacokinetics of a typical behaviorally active dose of 0.25–0.5 mg/kg by smoking or intravenous injection. Though we do not know the effects of chronic administration on methamphetamine pharmacokinetics, we showed in this study that a single administration of 0.2 mg/kg in an anesthetized baboon did not change the pharmacokinetics of ^{11}C-*d*-methamphetamine. Nonetheless, a prior study on mice showed that chronic methamphetamine administration significantly elevated the uptake of ^{11}C-methamphetamine and that uptake normalized after drug withdrawal (41). This finding can be examined in future studies on human methamphetamine abusers. We also note that prior studies on monkeys found an influence of different types of anesthesia on methamphetamine kinetics (12); thus, future studies on humans should assess methamphetamine kinetics in the awakened state.

CONCLUSION

Comparative PET studies showed no differences in brain pharmacokinetics between ^{11}C-*d*- and *l*-methamphetamine, suggesting that pharmacokinetics are unlikely to account for the different pharmacodynamic effects of the 2 enantiomers reported in humans and animals. Both enantiomers also showed rapid, high uptake and clearance in the heart, lungs, and kidneys and slower uptake and clearance in the liver and kidneys, possibly accounting for some of the toxic effects of methamphetamine in peripheral organs such as the heart and kidneys. Lack of pharmacologic blockade by methamphetamine indicates that the PET image represents

nonspecific binding, though the fact that methamphetamine is both a transporter *substrate* and an *inhibitor* may also play a role. A comparison of ^{11}C-*d*-methamphetamine and ^{11}C-(—)-cocaine in the same animal showed that the slower clearance of methamphetamine is likely to contribute to its previously reported (27) longer-lasting stimulant effects relative to those of (—)-cocaine. *d*-Methamphetamine and (—)-cocaine showed similar behavior in all peripheral organs examined except the kidneys and pancreas, which showed higher uptake for ^{11}C-*d*-methamphetamine, possibly accounting for the renal toxicity and pancreatic lesions reported in methamphetamine abusers. These studies set the stage for future studies using ^{11}C-*d*-methamphetamine as a tool to measure *d*-methamphetamine pharmacokinetics in humans.

ACKNOWLEDGMENTS

This research was carried out at Brookhaven National Laboratory under contract DE-AC02-98CH10886 with the U. S. Department of Energy and supported by its Office of Biological and Environmental Research and by NIH K05DA020001 and also in part by Deutscher Akademischer Austauschdienst (DAAD), Bonn, for a student fellowship for Carsten Kroll. We are grateful to Donald Warner and Michael Schueller for advice and assistance in different aspects of these studies.

REFERENCES

1. Barr AM, Panenka WJ, MacEqan W, et al. The need for speed: an update on MAMP addiction. J Psychiatry Neurosci 2006;31:301–313. [PubMed: 16951733]
2. Zhu JP, Xu W, Angulo JA. MAMP-induced cell death: selective vulnerability in neuronal subpopulations of the striatum in mice. Neuroscience 2006;140:607–622. [PubMed: 16650608]
3. Thompson PM, Hayashi KM, Simon KL, et al. Structural abnormalities in the brains of human subjects who use MAMP. J Neurosci 2004;24:6028–6036. [PubMed: 15229250]
4. Volkow ND, Chang L, Wang G-J, et al. Association of dopamine transporter reduction with psychomotor impairment in MAMP abusers. Am J Psychiatry 2001;158:377–382. [PubMed: 11229977]
5. Fitzmaurice PS, Tong J, Yazdanpanah M, Liu PP, Kalasinsky KS, Kish SJ. Levels of 4-hydroxynonenal and malondialdehyde are increased in brain of human chronic users of MAMP. J Pharmacol Exp Ther 2006;319:703–709. [PubMed: 16857724]
6. Mansergh G, Purcell DW, Stall R, et al. CDC consultation on MAMP use and sexual risk behavior for HIV/STD infection: summary and suggestions. Public Health Rep 2006;121:127–132. [PubMed: 16528944]
7. Mendelson J, Uemura N, Harris D, et al. Human pharmacology of the MAMP stereoisomers. Clin Pharmacol Ther 2006;80:403–420. [PubMed: 17015058]
8. Kuzcenski R, Segal DS, Cho AK, Melega W. Hippocampus norepinephrine, caudate dopamine and serotonin, and behavioral responses to the stereoisomers of amphetamine and methamphetamine. J Neurosci 1995;15:1308–1317. [PubMed: 7869099]
9. Cho AK. Ice: a new dosage form of an old drug. Science 1990;249:631–634. [PubMed: 17831955]
10. Inoue O, Axelsson S, Lundqvist H, Oreland L, Langstrom B. Effect of reserpine on the brain uptake of carbon 11 MAMP and its N-propargyl derivative, deprenyl. Eur J Nucl Med 1990;17:121–126. [PubMed: 2126235]
11. Shiue CY, Shiue GG, Cornish KG, O'Rourke MF. Comparative PET studies of the distribution of (—)-3,4-methylenedioxy-N-[^{11}C]MAMP and (—)-[^{11}C]MAMP in a monkey brain. Nucl Med Biol 1995;22:321–324. [PubMed: 7627147]
12. Mizugaki M, Nakagawa N, Nakamura H, et al. Influence of anesthesia on brain distribution of [^{11}C] methamphetamine in monkeys in positron emission tomography (PET) study. Brain Res 2001;911:173–175. [PubMed: 11511387]
13. Mizugaki M, Nakamura H, Hishinuma T, et al. Positron emission tomography (PET) study of the alterations in brain distribution of [^{11}C]MAMP in MAMP sensitized dog. Nucl Med Biol 1995;22:803–807. [PubMed: 8535342]

14. Ding YS, Lin KS, Logan J, et al. Comparative evaluation of positron emission tomography radiotracers for imaging the norepinephrine transporter: (S,S) and (R,R) enantiomers of reboxetine analogs ([^{11}C]methylreboxetine, 3-Cl-[^{11}C]methylreboxetine and [^{18}F]fluororeboxetine), (R)-[^{11}C] nisoxetine, [^{11}C]oxaprotiline and [^{11}C]lortalamine. J Neurochem 2005;94:337–351. [PubMed: 15998285]
15. Fowler JS, Volkow ND, Wolf AP, et al. Mapping cocaine binding sites in human and baboon brain in vivo. Synapse 1989;4:371–377. [PubMed: 2557686]
16. Logan J, Fowler JS, Volkow ND, et al. Graphical analysis of reversible radioligand binding from time-activity measurements applied to [N-^{11}C-methyl]-(—)-cocaine PET studies in human subjects. J Cereb Blood Flow Metab 1990;10:740–747. [PubMed: 2384545]
17. Alexoff DL, Shea C, Fowler JS, et al. Plasma input function determination for PET using a commercial laboratory robot. Nucl Med Biol 1995;22:893–904. [PubMed: 8547887]
18. Wilson AA, Jin L, Garcia A, DaSilva JN, Houle S. An admonition when measuring the lipophilicity of radiotracers using counting techniques. Appl Radiat Isot 2001;54:203–208. [PubMed: 11200881]
19. Dishino DD, Kilbourn MR, Raichle ME. Relationship between lipophilicity and brain extraction of C-11-labeled radiopharmaceuticals. J Nucl Med 1983;24:1030–1038. [PubMed: 6605416]
20. Black KJ, Snyder AZ, Koller JM, Gado MH, Perlmutter JS. Template images for nonhuman primate neuroimaging: 1. Baboon. Neuroimage 2001;14:736–743. [PubMed: 11506545]
21. Ding Y-S, Fowler JS, Volkow ND, et al. Pharmacokinetics and in vivo specificity of [^{11}C]dl-threo-methylphenidate for the presynaptic dopaminergic neuron. Synapse 1994;18:152–160. [PubMed: 7839313]
22. Dewey SL, Smith GS, Logan J, Brodie JD, Fowler JS, Wolf AP. Striatal binding of the PET ligand ^{11}C-raclopride is altered by drugs that modify synaptic dopamine levels. Synapse 1993;13:350–356. [PubMed: 8480281]
23. Volkow ND, Wang GJ, Fischman MW, et al. Relationship between subjective effects of cocaine and dopamine transporter occupancy. Nature 1997;386:827–830. [PubMed: 9126740]
24. Tsukada H, Miyasato K, Kakiuchi T, et al. Comparative effects of MAMP and nicotine on the striatal [(^{11})C]raclopride binding in unanesthetized monkeys. Synapse 2002;45:207–212. [PubMed: 12125041]
25. Ritz MC, Lamb RJ, Goldberg SR, Kuhar MJ. Cocaine receptors on dopamine transporters are related to self-administration of cocaine. Science 1987;237:1219–1223. [PubMed: 2820058]
26. Ding YS, Fowler JS, Logan J, et al. 6-[^{11}F]Fluoro-A-85380, a new PET tracer for the nicotinic acetylcholine receptor: studies in the human brain and in vivo demonstration of specific binding in white matter. Synapse 2004;53:184–189. [PubMed: 15236351]
27. Newton TF, Roache JD, De La Garza R III, et al. Buproprion reduces MAMP-induced subjective effects and cue-induced craving. Neuropsychopharmacology 2006;31:1537–1544. [PubMed: 16319910]
28. Fowler JS, Volkow ND, Wolf AP, et al. Mapping cocaine binding sites in human and baboon brain in vivo. Synapse 1989;4:371–377. [PubMed: 2557686]
29. Caldwell J, Dring LG, Williams RT. Metabolism of [^{14}C]MAMP in man, the guinea pig and the rat. Biochem J 1972;129:11–22. [PubMed: 4646771]
30. Gatley SJ, Yu DW, Fowler JS, et al. Studies with differentially labeled [^{11}C]cocaine, [^{11}C]norcocaine, [^{11}C]benzoylecgonine, and [^{11}C]- and 4'-[^{18}F] fluorococaine to probe the extent to which [^{11}C] cocaine metabolites contribute to PET images of the baboon brain. J Neurochem 1994;62:1154–1162. [PubMed: 8113802]
31. Yamamoto BK, Bankson MG. Amphetamine neurotoxicity: cause and consequence of oxidative stress. Crit Rev Neurobiol 2005;17:87–118. [PubMed: 16808729]
32. Yu Q, Larson DF, Watson RR. Heart disease, MAMP and AIDS Review. Life Sci 2003;73:129–140. [PubMed: 12738029]
33. Yeo KK, Wijetunga M, Ito H, et al. The association of methamphetamine use and cardiomyopathy in young patients. Am J Med 2007;120:165–171. [PubMed: 17275458]
34. Volkow ND, Fowler JS, Wolf AP, et al. Distribution and kinetics of carbon-11-cocaine in the human body measured with PET. J Nucl Med 1992;33:521–525. [PubMed: 1552335]

35. Fowler JS, Ding YS, Volkow ND, et al. PET studies of cocaine inhibition of myocardial norepinephrine uptake. Synapse 1994;16:312–317. [PubMed: 8059340]

36. Tokunaga I, Kubo S, Ishigami A, Gotohda T, Kitamura O. Changes in renal function and oxidative damage in methamphetamine-treated rat. Leg Med (Tokyo) 2006;8:16–21. [PubMed: 16157497]

37. Ishigami A, Tokunaga I, Gotohda T, Kubo S. Immunohistochemical study of myoglobin and oxidative injury-related markers in the kidney of methamphetamine abusers. Leg Med (Tokyo) 2003;5:42–48. [PubMed: 12935649]

38. Ito Y, Jono H, Shojo H. A histopathological study of pancreatic lesions after chronic administration of MAMP to rats. Kurume Med J 1997;44:209–215. [PubMed: 9339652]

39. Souza F, Simpson N, Raffo A, et al. Longitudinal noninvasive PET-based beta cell mass estimates in a spontaneous diabetes rat model. J Clin Invest 2006;116:1506–1513. [PubMed: 16710474]

40. McMahon EM, Andersen DK, Feldman JM, Schanberg SM. MAMP-induced insulin release. Science 1971;174:66–68. [PubMed: 5120870]

41. Mizugaki M, Hishinuma T, Nakamura H, et al. Distribution of carbon-11 labeled MAMP and the effect of its chronic administration in mice. Nucl Med Biol 1993;20:487–492. [PubMed: 8504290]

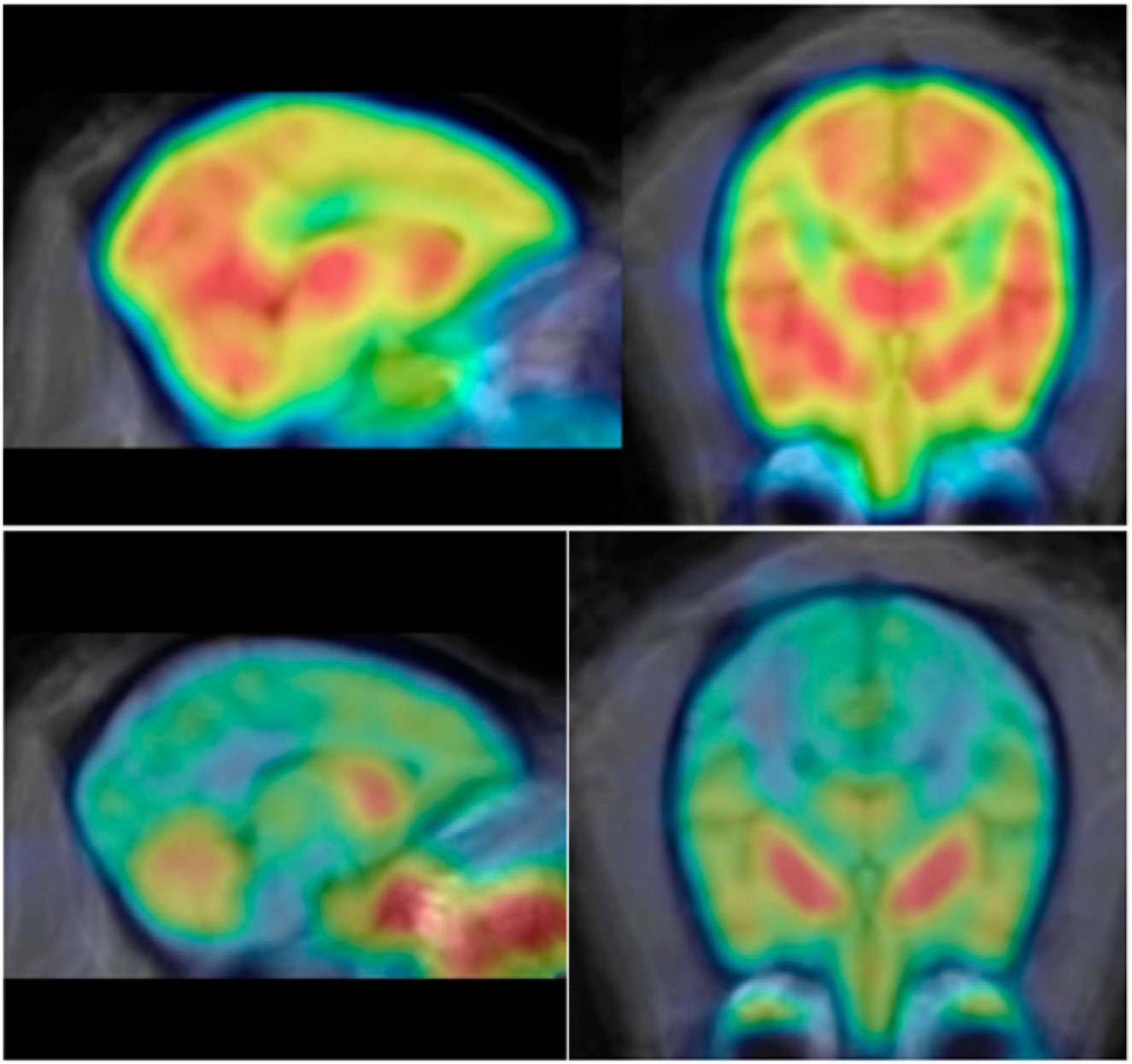

FIGURE 1.
Summed brain images for ^{11}C-*d*-methamphetamine (top row, from 0–90 min) and ^{11}C-*l*-(—)-cocaine (bottom row, from 0–54 min) in same animal. ^{11}C distribution is widespread over cortical and subcortical brain regions for ^{11}C-*d*-methamphetamine but is highly localized in striatum for ^{11}C-(—)-cocaine. Images are coregistered to MRI atlas (20).

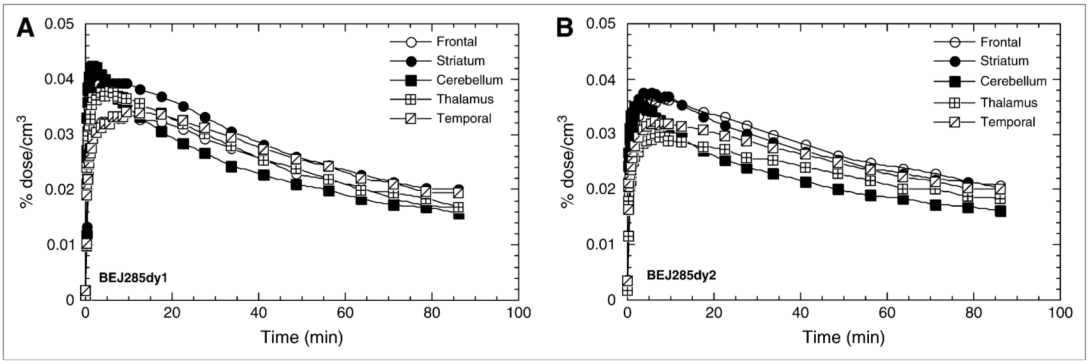

FIGURE 2.

Time—activity curves for cortical and subcortical brain regions for ^{11}C-*d*-methamphetamine (A) and ^{11}C-*l*-methamphetamine (B) in same baboon (BEJ285dy1 and BEJ285dy2 refer to study number). Brain kinetics are similar for different brain regions.

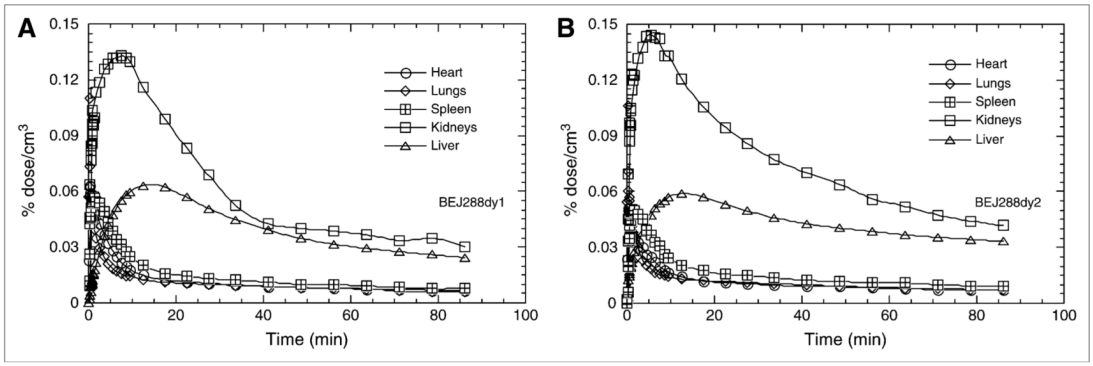

FIGURE 3.

Comparison of ^{11}C-*d*-methamphetamine (A) and ^{11}C-*l*-methamphetamine (B) distribution in peripheral organs in baboon (BEJ288dy1 and BEJ288dy2 refer to study number). ^{11}C distribution is similar for the 2 enantiomers.

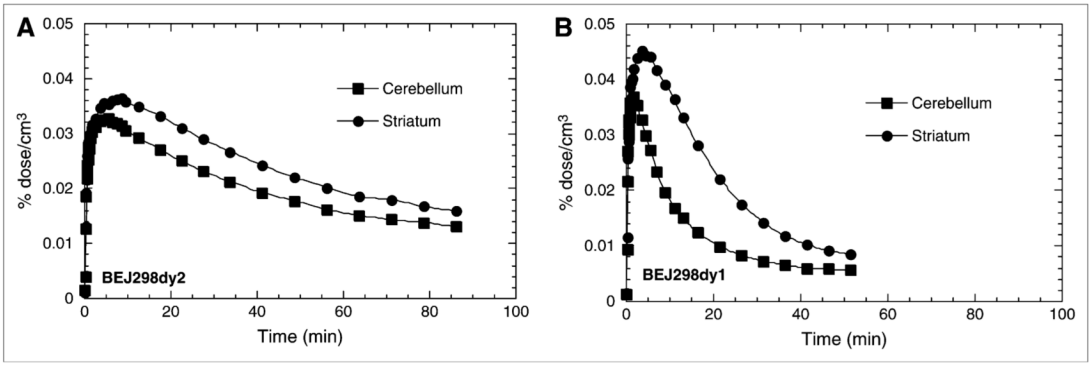

FIGURE 4.

Time—activity curves for ^{11}C-*d*-methamphetamine (A) and ^{11}C-(—)-cocaine (B) in cerebellum and striatum in same baboon (BEJ298dy1 and BEJ298dy2 refer to study number). Clearance of ^{11}C-*d*-methamphetamine is lower and slower than that of ^{11}C-(—)-cocaine.

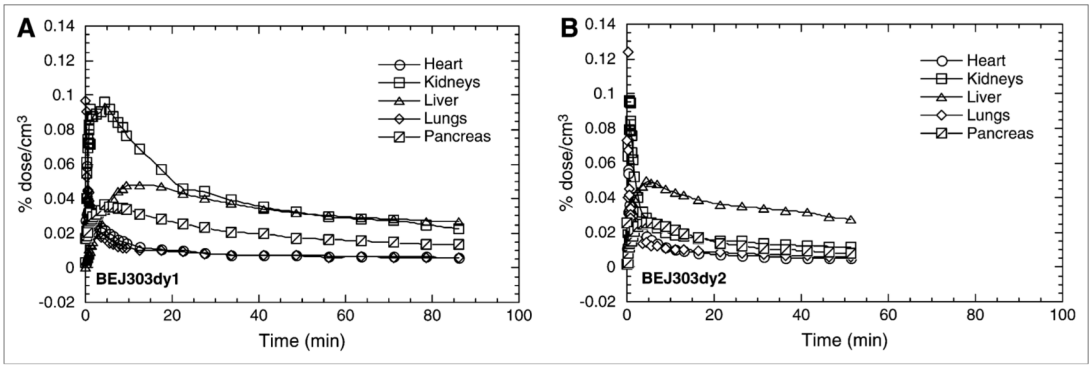

FIGURE 5.

Comparison of distribution and clearance of ^{11}C-*d*-methamphetamine (A) and ^{11}C-(—)-cocaine (B) in peripheral organs in same baboon (BEJ303dy1 and BEJ303dy2 refer to study number). Both compounds show similar distribution and kinetics in heart, lungs, and liver, but *d*-methamphetamine has much greater uptake and slower clearance in kidneys and higher uptake in pancreas than does ^{11}C-(—)-cocaine.

TABLE 1

Summary of Baboon PET Studies

Study no.	Baboon's name	Radiotracer	Location	Drug treatment
d vs. *l*				
BEJ284dy1,2	Spicey	*l* (run 1); *d* (run 2)	Brain	None
BEJ285dy1,2	Friendly	*d* (run 1); *l* (run 2)	Brain	None
BEJ307dy1,2	Daisy	*d* (run 1); *l* (run 2)	Brain	None
BEJ288dy1,2	Daisy	*d* (run 1); *l* (run 2)	Torso	None
BEJ290dy1,2	Chloe	*l* (run 1); *d* (run 2)	Torso	None
d vs. drug treatment				
BEJ280dy1,2	Daisy	*d* (run 1); *d* (run 2)	Brain	None
BEJ287dy1,2	Missy	*d* (run 1); *d* (run 2)	Brain	Baseline; *d*-methamphetamine, 0.2 mg/kg intravenously, 5 min prior
BEJ291dy1,2	Pearl	*d* (run 1); *d* (run 2)	Brain	Baseline; methylphenidate, 0.5 mg/kg intravenously, 10 min prior
BEJ329dy1,2	Spicey	*d* (run 1); *d* (run 2)	Brain	Baseline; tetrabenazine; 4 mg/kg intravenously, 60 min prior
d vs. 11C-(2)-cocaine				
BEJ303dy1,2	Friendly	*d* (run 1); cocaine (run 2)	Torso	None
BEJ298dy1,2	Missy	Cocaine (run 1); *d* (run 2)	Brain	None

d = ^{11}C-*d*-methamphetamine; *l* = ^{1}C-*l*-methamphetamine.

TABLE 2

Comparison of Data for Striatum and Cerebellum

Parameter	^{11}C-*d*-methamphetamine	^{11}C-*l*-methamphetamine
% dose/cm^3 (peak)		
Striatum	0.033 ± 0.008	0.036 ± 0.003
Cerebellum	0.034 ± 0.01	0.034 ± 0.004
Peak time (min)		
Striatum	7.2 ± 2.3	7.5 ± 2.6
Cerebellum	4.5 ± 4.5	4.5 ± 1.5
Clearance half-time from peak (min)		
Striatum	80.3 ± 18.6	98.5 ± 22.3
Cerebellum	59.3 ± 18.3	67.5 ± 12.3
DVR (Striatum:cerebellum)	1.22 ± 0.04	1.22 ± 0.027
Plasma integral for total ^{11}C at 60 min*	2,411 ± 399 (1,348 ± 33)	1,833 ± 203 (1,351 ± 51)

*There was a trend toward greater ^{11}C in plasma at 60 min for *d*-enantiomer ($P < 0.08$). Data in parentheses are fraction of ^{11}C as methamphetamine (mean ± SD, $n = 3$).

J Nucl Med. Author manuscript; available in PMC 2009 August 26.

TABLE 3

Comparison of Fraction of Total ^{11}C in Plasma That Is Present as Parent Radiotracer at Different Times After Injection

Time (min)	^{11}C-*d*-methamphetamine (*n* = 9)	^{11}C-*l*-methamphetamine (*n* = 3)	P
2	93 ± 2.4	95 ± 2	NS
5	83 ± 5	89 ± 2.3	0.06
10	69.9 ± 6.8	82.3 ± 3.5	0.01
20	53.4 ± 8.5	72 ± 6.2	0.006
30	44.4 ± 8.5	67 ± 9.6	0.003
60	32.3 ± 7.7	58.7 ± 13.05	0.002
90	26.9 ± 6.4	49 ± 17	0.01

NS = not statistically significant.

TABLE 4

Comparison of DVRs at Baseline and After Drug Treatment for ^{11}C-*d*-Methamphetamine

Drug	DVR (baseline)	DVR (after treatment)	% Change
Control	1.21	1.28	+5
d-Methamphetamine	1.19	1.16	-2
Methylphenidate	1.28	1.19	-7
Tetrabenazine	1.18	1.24	+5